EXECUTIVE SUMMARY OF THE THESIS

Divertor heat flux and scrape-off layer turbulence studies in negative and positive triangularity plasmas in the TCV tokamak

LAUREA MAGISTRALE IN NUCLEAR ENGINEERING - INGEGNERIA NUCLEARE

Author: RICCARDO IAN MORGAN

Advisor: PROF. MATTEO PASSONI

Co-advisors: PROF. CHRISTIAN G. THEILER, DR. THEODORE GOLFINOPOULOS

Academic year: 2023-2024

1. Introduction

Nuclear fusion, the energy source of all active stars in the universe, is a promising candidate for future power plants since, compared to present-day alternatives, it offers a cleaner, safer and potentially unlimited source of energy. In particular, when two hydrogen nuclei get close enough, they can fuse together into helium, liberating a vast amount of energy in the process. To date, the best candidate to harness this energy is a machine called Tokamak: a toroidal chamber in which an extremely hot plasma is kept confined by strong magnetic fields.

1.1. Tokamak magnetic field

The magnetic field has a strong component in the toroidal direction (revolving around the torus) and another, weaker, component in the poloidal plane (the cross section perpendicular to the toroidal direction, shown in Fig.1; any poloidal cross-section is equivalent to the others, due to the tokamak axisymmetry). The former is generated by external field coils, the latter by a current induced into the plasma itself. The resulting field lines wrap themselves indefinitely around the torus, creating a collection of nested magnetic surfaces (or *flux surfaces*).
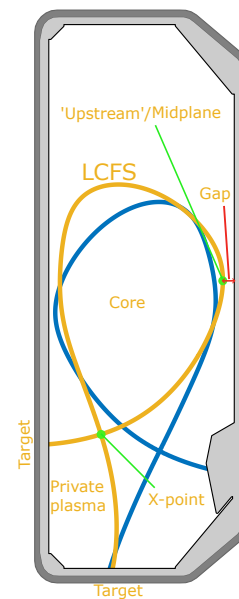

Figure 1: Poloidal cross section of a typical TCV plasma. Blue: NT; yellow: PT.

Inside the *Last Closed Flux Surface* (LCFS), all such surfaces are closed, meaning that plasma particles (which move following the magnetic field lines) are well confined. However, if particles cross the LCFS, they enter a region called *Scrape-Off Layer* (SOL), in which density and temperature quickly drop. In fact, particles

1

would be moving along field lines that pass through the machine walls and they would soon slam into them.

As a consequence, extremely intense heat fluxes are expected on this exposed region of the wall, known as *divertor*.

1.2.   Heat fluxes and detachment

If next to the plasma core (*upstream*), this parallel heat flux has a roughly exponential profile, while it travels towards the divertor target it can spread due to diffusion processes, especially when it passes past the *X-point* and finds itself next to the colder and less dense *private plasma*. The final profile (scattered in Fig.2) is usually well described by a function proposed by Eich [1]:

$$q_{||}(\bar{s}) = \frac{q_0}{2} e^{\left(\frac{S}{2\lambda_q}\right)^2 - \frac{\bar{s}}{\lambda_q}} \operatorname{erfc}\left(\frac{S}{2\lambda_q} - \frac{\bar{s}}{S}\right) + q_{bg} \qquad (1)$$

where $\bar{s}$ is a coordinate following the divertor target, q_0 is a proportionality constant, S describes the flux diffusion and λ_q quantifies the fall-off length.

This last parameter is very important, since it describes how big of a surface the heat flux is spread over. Lower λ_q values would lead to higher fluxes being concentrated on a narrower region and are thus undesirable. Over time, many scaling laws have been published to predict λ_q with the highest possible accuracy.

Sometimes a second peak is visible in the heat flux profile, not predicted by the Eich model. In the literature it has been partially explained with drift phenomena.

The usual approach to deal with intense heat fluxes is to operate the divertor in a *detached* regime. This happens when the plasma temperature in the SOL, close to the target, gets low enough that charge recombination can take place: then, a high generation of neutral atoms creates a "cushion" between the plasma and the divertor in which a lot of energy is dispersed in a radiative way. The heat flux to the divertor is then strongly reduced.

1.3.   SOL Filamentary turbulence

The SOL is interested by the frequent expulsion of structures made of denser and hotter plasma. These filaments can be very extended ($\approx$ m) along the magnetic field direction, while on the poloidal cross-section they appear like ellipsoids

with much smaller dimensions ($\approx$ cm): for this reason, they are known as *blobs*.

The denser and hotter nature of blobs, along with the fact that they are expelled across the SOL with very high velocity ($\approx$ 1km/s), makes their effect on the plasma heat exhaust not negligible, especially far from the LCFS.

The driving force of the blobs radial motion is the $\mathbf{E} \times \mathbf{B}$ drift, arising due to the electric field inside the blob (generated by charge separation) coupling with the strong tokamak magnetic field.

1.4.   Plasma confinement

Magnetically confined plasmas can exist in different "regimes", according to their confinement level. *H-mode* plasmas can generally confine particles and energy for longer time. This benefit comes however at a cost: very strong density and temperature gradients develop across the LCFS and can become so steep to cyclically break and release intense outbursts of energy known as *Edge Localized Modes* (ELMs) that could bring much harm to the vessel walls.

L-mode plasmas are intrinsically ELM-free, but they are associated with lower confinement times.

1.5.   Triangularity

Over time, research on plasma shaping led to identify *triangularity* (δ) as a crucial parameter. δ describes, for positive values (PT), the distortion of the plasma cross-section into a "D", while negative values (NT) result in a "reverse-D" shape (Fig.1).

NT shapes have been recently associated with various beneficial effects, including higher L-mode confinement level and lower filamentary turbulence in the SOL [3]; however, also deleterious effects have been observed, first of all the reduction of the heat flux fall-off length λ_q [2].

1.6.   Motivation,   objectives   and   methods

These results have reopened the question whether future devices should operate in PT or NT configurations. This thesis is devoted to further investigate the plasma edge in both scenarios focusing on divertor heat flux and SOL filamentary turbulence. A possible connection between these phenomena is also proposed in the

form of a heuristic blob model.

This thesis fits into the line of research on the physics of the plasma edge, contributing to a higher level of comprehension of the complex phenomena taking place in this region. Ultimately, these efforts will prove important in the design of fusion power plants.

The work has an experimental nature: all data have been obtained from the TCV tokamak, located in the École polytechnique fédérale de Lausanne (EPFL) university in Lausanne, Switzerland. Data collected by the tokamak diagnostics were then processed by MATLAB routines (some of which were specifically written for this thesis) to extract the physical quantities presented here and to investigate possible correlations among them.

In order to conduct this work, I spent 5 months at EPFL to get acquainted with the subject and to access TCV data, followed by 1 month at the Massachusetts Institute of Technology (MIT), Boston, USA.

2. TCV and diagnostics

The exceptional plasma shaping capabilities of the Tokamak à Configuration Variable (TCV) made it the leading tokamak in NT studies over the past 30 years. To collect experimental data, TCV exploits several diagnostics: the main ones used in this thesis are explained in the following.

2.1. Gas-Puff Imaging

GPI is a diagnostic commissioned for the study of turbulent phenomena in the SOL. It relies on neutral atoms that, puffed into the vessel, come in contact with the plasma, get excited and emit visible light, which is redirected on a camera by an optical system.

Two GPI systems are installed on TCV: one inspecting the outer midplane, the other focused on the X-point region. Both have an acquisition frequency ($\approx 0.4-2$ MHz) high enough to detect all rapidly passing blobs, whose light brightness will be higher than the background.

At this point, data is processed by a *Conditional Average Sampling* (CAS) algorithm which retrieves the average properties (size and velocity) of blobs passing in the location of a trigger point over a quite long time window.

2.2. Langmuir Probes

LPs on TCV are graphite cylinders embedded into the vessel wall, including the divertor target. During operation, a time-dependent voltage is applied between them and the wall, so that they collect a net current through the plasma. This allows to capture the current-potential curve, and to fit it with an appropriate physical model to retrieve the local plasma parameters, such as density and temperature.

Finally, the acquired information allows to reconstruct the heat and particle fluxes to the divertor with a sampling frequency of ≈ 100 Hz.

2.3. Other diagnostics

A Far-InfraRed interferometer (FIR) is used to acquire a vertically line-averaged plasma density.

Baratron gauges are exploited to measure the neutral atoms pressure in the divertor region.

A multi-spectral camera system (MANTIS) is used to reconstruct a 2D poloidal view of the Carbon-3 impurity radiation, useful in the determination of a detached divertor regime.

3. Results

To assess the role of triangularity, I collected ≈ 100 TCV shots in which all the other parameters do not change too much. As a preliminary work, the shots were analyzed to ensure that they were within the boundaries of L-mode, operation with attached divertor. Doing this required to check the trends of various plasma parameters such as the line-average density, the D_α radiation levels, the particle flux to the divertor target, the neutrals pressure and the position of the C-III impurity emission front.

Results confirmed that all shots were operating in L-mode. To ensure the permanence in attached conditions, a density upper limit was identified at $4.5 \cdot 10^{19} \mathrm{m}^{-3}$: all further analysis will be limited to plasma shots below this value.

3.1. Divertor heat flux

For each shot, LP data from a suitable time window was collected, rescaled to "upstream" conditions and fitted with an Eich function, sometimes excluding data if a second peak was visible (Fig.2).

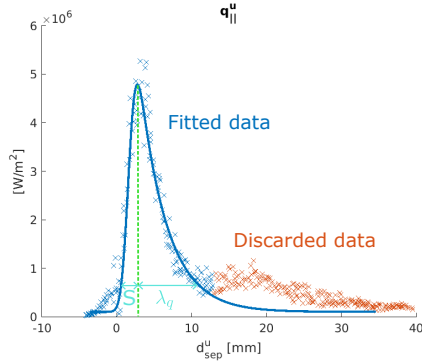A comparison between λ_q scaling laws (especially the ones featuring triangularity) and ex-

Figure 2: Example of Eich fit, ignoring the second peak. The physical meaning of S and λ_q is also shown (the lengths drawn on the figure are indicative and do not represent the definitions of S and λ_q).

perimental data was then possible. In Fig.3, λ_q is plotted against the total, upper and lower triangularity (δ, δ_u, δ_l). The strongest dependence is clearly the one on δ_u, that justifies the milder dependence on δ, in a picture in which δ_l looks unimportant. The horizontal dashed lines represent λ_q predictions of the δ-independent scaling laws, which overall give a fairly reasonable estimate of the experimental values. Lim's and Horacek's E3 correlations depend respectively on δ and δ_u. The former is by far the best, among all considered scaling laws.
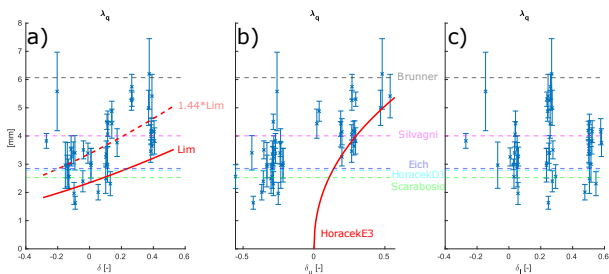

Figure 3: Comparison of λ_q scaling laws and experimental data. Dashed horizontal lines are correlations not depending on triangularity. Data is plotted against δ (a), δ_u (b), δ_l (c).

The spreading factor S (whose value is spread in the interval $0.5 - 3.5$ mm) is not found to be affected by triangularity. In fact, linear regressions were performed against a high number of plasma parameters and none of them returned R^2 values higher than 0.1, indicating that S is either unaffected, or the result of a more complex interaction among them.

The trend of q_0 with δ_u is shown in Fig.4. The

colour code highlights the role of the toroidal field direction. We can notice higher q_0 values for reverse field shots, together with an unexpected spreading for the lowest triangularity. Also, we can notice how the error bars become wider as δ_u gets lower.
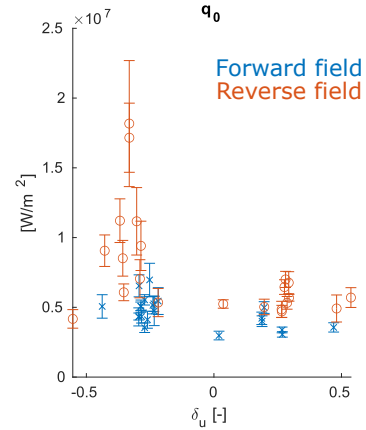

Figure 4: q_0 against δ_u.

The q_0 increase for lower δ_u was found compatible with the fact that the integral of the divertor heat flux (observed to be independent of triangularity) is given by $q_0\lambda_q$. The unexplained observation that forward field plasmas radiate more energy from the core, can explain the lower q_0 values registered in this scenario.

The widening of the error bars could be explained considering that the lower values of λ_q associated with lower triangularity, would generate a narrower peak. Uncertainties in equilibrium reconstruction and heat flux computation, concentrated in a smaller region, would give a less clear profile, thus making a good fit more difficult.

Finally, the particle flux was chosen to investigate the second peak, since such a feature is found to be more visible there, rather than in the heat flux profile. A regression analysis with a number of plasma parameters found that the position of the second peak moves radially outwards when increasing the width of the *outer gap* (distance between the LCFS at midplane and the outer wall, see Fig.1).

4. SOL filamentary turbulence

Blobs were studied in the SOL with GPI. A first analysis of the light brightness fluctuations, conducted with the midplane GPI system, confirmed the role of negative triangularity in tur-

bulence suppression.

Then, to study the average blob behaviour, a CAS analysis was performed, with evenly distributed trigger points. The most noticeable result was a discrepancy in the blobs poloidal size, with strongly shaped plasmas (both in NT and PT) having smaller blobs, highlighting once again the role of plasma shaping in turbulence control and thus confinement improvement.

The same analyses described here were repeated with the X-point GPI data, this time comparing shots with upper triangularity δ_u changing from positive to negative, while δ_l was fixed. The CAS analysis confirmed the same poloidal size trends seen in the midplane case, but above all showed a difference in the profiles of the blobs radial velocity v_r (Fig.5): while close to the LCFS slower blobs were detected (some even moving towards the core), higher velocities are reached further in the SOL, where a peak can be distinguished before v_r starts decreasing again. We notice that upper PT blobs (yellow) reach peak velocities of ≈ 1 km/s, while the upper NT blobs (orange) reach more modest values, around ≈ 0.6 km/s, before slowing down.
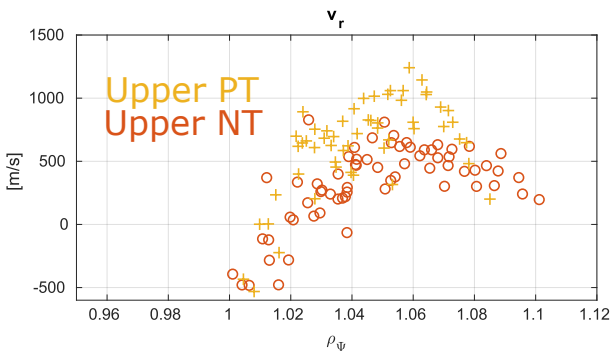

Figure 5: Blobs v_r in the X-point region. On the x axis: a radial coordinate in which 1 is the LCFS position.

The reason behind the blobs slowing down could be related to the width of the outer gap: recalling that blobs can be very extended in the parallel-to-$\mathbf{B}$ direction, the blob portion at the outer midplane is formed already very close to the wall. Its outwards movement will soon put it in contact with the vessel, thus creating a good path for currents to flow and resulting in current closure. The consequent decrease of the blob electric field would reduce the $\mathbf{E} \times \mathbf{B}$ drift and slow the blob down.

4.1. Heuristic blob model

A simple heuristic blob model was proposed to investigate a possible connection between the results obtained so far. The basic hypothesis of the model is that the heat and particle fluxes to the divertor are the result of two separate contributions: the unperturbed SOL (in the ideal case in which no blobs are generated) and the blobs themselves. The former is described by an ideal Eich function, the latter are simulated by very simplified fluid equations and their contribution is weighted on the *packing fraction* (percentage of time in which a blob is covering a certain position on the divertor).

When possible, as in the case of the blobs, the parameters for running the model were taken from experimental data; however some quantities remained (to this stage) not measurable, such as the parameters defining an ideally unperturbed SOL: these were conveniently chosen (within the boundaries of reasonable values) so that the final results would resemble experimental data. As a consequence, we should focus more on qualitative results, rather than quantitative conclusions.

The main reason for creating this model was to test the following hypothesis: the observed influence of triangularity on λ_q and other features of the heat flux profile is mediated by the blobs behaviour, seen to depend on triangularity as well. We can imagine in fact that blobs with higher v_r (PT case) would transport energy outwards more efficiently, thus relaxing the heat flux profile decay and resulting in a higher λ_q. Also, the observed v_r profiles describe a scenario in which blobs travel fast across the SOL, but then slow down, thus delivering more energy to an almost fixed position on the target: this mechanism is proposed as an alternative (and complementary) explanation of the second peak insurgence.

The model was indeed successful in reproducing many experimental observations, including the ones just described. In particular, when simulating blobs with fixed v_r, it could reproduce the insurgence in the heat flux profile of a slowly-decaying tail and (partially) the increase of λ_q. When introducing in the model the realistic v_r profile shown in Fig.5, the model could reproduce the insurgence of a second peak, confirming its higher visibility in the particle flux profile, rather than in the heat flux one (Fig.6). This

final observation was explained by the model prediction of a second peak in the density profile, but not in the temperature one. Since temperature has a much stronger role in computing the heat flux, the density's second peak is more strongly mitigated.
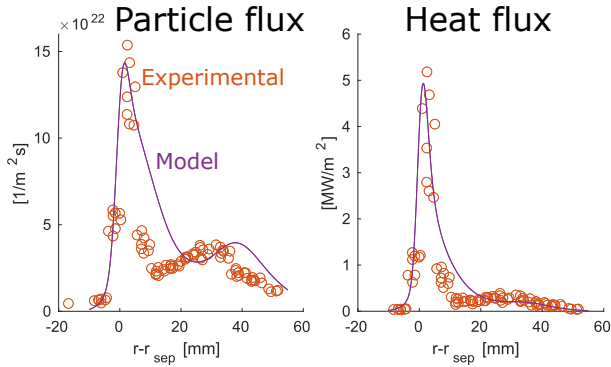

Figure 6: Experimental data (orange) and model computation (purple).

5.   Conclusions

This thesis investigated the role of triangularity on crucial SOL phenomena through the analysis of a high number of L-mode, attached shots from the TCV tokamak. For each shot, the heat flux profile on the divertor target was retrieved via Langmuir Probe measurements and fitted with an Eich profile. The fall-off length λ_q was observed to steadily decrease for decreasing upper triangularity δ_u. The importance of triangularity as a parameter for good scaling laws was also highlighted. Issues with the q_0 estimation were shown and explained to some extent. Some of them were indicated as consequences of the λ_q variation with triangularity. An investigation of the second peak in divertor fluxes linked its position to the width of the outer gap.

Through the development of a heuristic blob model, most of these results were found compatible with the observed behaviour of turbulent blobs in the SOL, in turn dependent on triangularity. In particular, the blobs radial velocity v_r was identified as the link between these phenomena.

Along the work, many possibilities of future research have been identified: a non-comprehensive list includes the broadening of this work to larger triangularity ranges, the study of the dependency on input power of the Eich fitting parameters, the investigation of the

change in radiated power with the inversion of the magnetic field, the combined role of drifts and blobs in the second peak position, a novel approach to Eich fitting itself, a more detailed development of the heuristic blob model and more.

6.   Acknowledgements

References

[1] T. Eich, B. Sieglin, A. Scarabosio, W. Fundamenski, R. J. Goldston, A. Herrmann, and ASDEX Upgrade Team. Inter-ELM Power Decay Length for JET and ASDEX Upgrade: Measurement and Comparison with Heuristic Drift-Based Model. *Physical Review Letters*, 107(21):215001, November 2011.

[2] M Faitsch, R Maurizio, A Gallo, S Coda, T Eich, B Labit, A Merle, H Reimerdes, B Sieglin, C Theiler, the Eurofusion MST1 Team, and the TCV Team. Dependence of the L-Mode scrape-off layer power fall-off length on the upper triangularity in TCV. *Plasma Physics and Controlled Fusion*, 60(4):045010, April 2018.

[3] W. Han, N. Offeddu, T. Golfinopoulos, C. Theiler, C.K. Tsui, J.A. Boedo, E.S. Marmar, and The Tcv Team. Suppression of first-wall interaction in negative triangularity plasmas on TCV. *Nuclear Fusion*, 61(3):034003, March 2021.